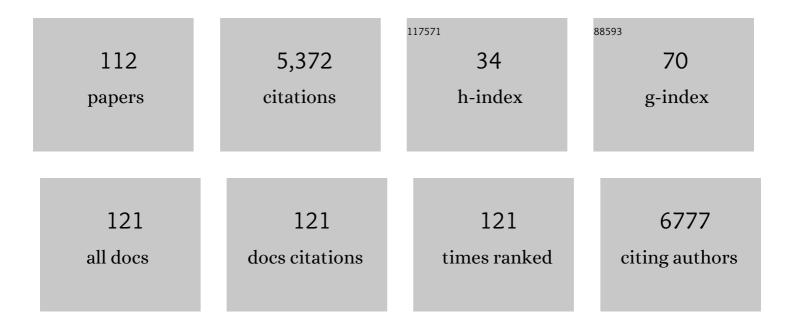
Hiroyuki Asakura

List of Publications by Year in descending order

Source: https://exaly.com/author-pdf/694346/publications.pdf Version: 2024-02-01



ΗΙΡΟΥΙΙΚΙ Δελκιιρλ

#	Article	IF	CITATIONS
1	Effect of the in situ addition of chromate ions on H2 evolution during the photocatalytic conversion of CO2 using H2O as the electron donor. Catalysis Today, 2023, 410, 273-281.	2.2	1
2	In situ time-resolved XAS study on metal-support-interaction-induced morphology change of PtO2 nanoparticles supported on γ-Al2O3 under H2 reduction. Catalysis Today, 2022, , .	2.2	3
3	Formation of CH ₄ at the Metalâ€Support Interface of Pt/Al ₂ O ₃ During Hydrogenation of CO ₂ : <i>Operando</i> XASâ€DRIFTS Study. ChemCatChem, 2022, 14, .	1.8	7
4	Oxygen Storage Capacity of Co-Doped SrTiO ₃ with High Redox Performance. Journal of Physical Chemistry C, 2022, 126, 4415-4422.	1.5	7
5	Identifying Key Descriptors for the Single-Atom Catalyzed CO Oxidation. CCS Chemistry, 2022, 4, 3296-3308.	4.6	25
6	Dynamic behavior of Pd/Ca2AlMnO5+l̂´for purifying automotive exhaust gases under fluctuating oxygen concentration. Catalysis Today, 2022, , .	2.2	0
7	Design, Identification, and Evolution of a Surface Ruthenium(II/III) Single Site for CO Activation. Angewandte Chemie - International Edition, 2021, 60, 1212-1219.	7.2	8
8	Effect of Ligand on the Electronic State of Gold in Ligand-Protected Gold Clusters Elucidated by X-ray Absorption Spectroscopy. Journal of Physical Chemistry C, 2021, 125, 3143-3149.	1.5	10
9	Real-time observation of the effect of oxygen storage materials on Pd-based three-way catalysts under ideal automobile exhaust conditions: an <i>operando</i> study. Catalysis Science and Technology, 2021, 11, 6182-6190.	2.1	9
10	Dual Ag/Co cocatalyst synergism for the highly effective photocatalytic conversion of CO ₂ by H ₂ O over Al-SrTiO ₃ . Chemical Science, 2021, 12, 4940-4948.	3.7	34
11	The Electrophilicity of Surface Carbon Species in the Redox Reactions of CuO eO 2 Catalysts. Angewandte Chemie, 2021, 133, 14541-14549.	1.6	2
12	The Electrophilicity of Surface Carbon Species in the Redox Reactions of CuO eO ₂ Catalysts. Angewandte Chemie - International Edition, 2021, 60, 14420-14428.	7.2	24
13	Oxygen Release and Storage Property of Fe–Al Spinel Compounds: A Three-Way Catalytic Reaction over a Supported Rh Catalyst. ACS Applied Materials & Interfaces, 2021, 13, 24615-24623.	4.0	4
14	Recent Applications of X-ray Absorption Spectroscopy in Combination with High Energy Resolution Fluorescence Detection. Chemistry Letters, 2021, 50, 1075-1085.	0.7	6
15	Local Structure and L ₁ - and L ₃ -Edge X-ray Absorption Near Edge Structures of Middle Lanthanoid Elements (Eu, Gd, Tb, and Dy) in Their Complex Oxides. Inorganic Chemistry, 2021, 60, 9359-9367.	1.9	8
16	Frontispiz: The Electrophilicity of Surface Carbon Species in the Redox Reactions of CuO eO ₂ Catalysts. Angewandte Chemie, 2021, 133, .	1.6	0
17	Ionic Liquid-Stabilized Single-Atom Rh Catalyst Against Leaching. CCS Chemistry, 2021, 3, 1814-1822.	4.6	30
18	Strong Metal–Support Interaction in Pd/Ca2AlMnO5+Î′: Catalytic NO Reduction over Mn-Doped CaO Shell. ACS Catalysis, 2021, 11, 7996-8003.	5.5	9

#	Article	IF	CITATIONS
19	Frontispiece: The Electrophilicity of Surface Carbon Species in the Redox Reactions of CuO eO ₂ Catalysts. Angewandte Chemie - International Edition, 2021, 60, .	7.2	1
20	NO _{<i>x</i>} Storage Performance at Low Temperature over Platinum Group Metal-Free SrTiO ₃ -Based Material. ACS Applied Materials & Interfaces, 2021, 13, 29482-29490.	4.0	9
21	Highly Selective Photocatalytic Conversion of Carbon Dioxide by Water over Al-SrTiO ₃ Photocatalyst Modified with Silver–Metal Dual Cocatalysts. ACS Sustainable Chemistry and Engineering, 2021, 9, 9327-9335.	3.2	26
22	Development of Zinc Hydroxide as an Abundant and Universal Cocatalyst for the Selective Photocatalytic Conversion of CO 2 by H 2 O. ChemCatChem, 2021, 13, 4313.	1.8	4
23	Shift of active sites via in-situ photodeposition of chromate achieving highly selective photocatalytic conversion of CO2 by H2O over ZnTa2O6. Applied Catalysis B: Environmental, 2021, 298, 120508.	10.8	9
24	Effect of Zn in Ag-Loaded Zn-Modified ZnTa ₂ O ₆ for Photocatalytic Conversion of CO ₂ by H ₂ O. Journal of Physical Chemistry C, 2021, 125, 1304-1312.	1.5	10
25	Preparation of partial crystalline mesoporous zeolite TS-1 for epoxidation of unsaturated fatty acid ester. Catalysis Today, 2020, 355, 180-187.	2.2	5
26	xTunes: A new XAS processing tool for detailed and on-the-fly analysis. Radiation Physics and Chemistry, 2020, 175, 108270.	1.4	36
27	Promotional Effect of La in the Three-Way Catalysis of La-Loaded Al ₂ O ₃ -Supported Pd Catalysts (Pd/La/Al ₂ O ₃). ACS Catalysis, 2020, 10, 1010-1023.	5.5	46
28	Catalytic Production of Alanine from Waste Glycerol. Angewandte Chemie, 2020, 132, 2309-2313.	1.6	18
29	Catalytic Production of Alanine from Waste Glycerol. Angewandte Chemie - International Edition, 2020, 59, 2289-2293.	7.2	84
30	Enhanced CO evolution for photocatalytic conversion of CO2 by H2O over Ca modified Ga2O3. Communications Chemistry, 2020, 3, .	2.0	26
31	Zeoliteâ€Encaged Pd–Mn Nanocatalysts for CO ₂ Hydrogenation and Formic Acid Dehydrogenation. Angewandte Chemie, 2020, 132, 20358-20366.	1.6	22
32	Zeoliteâ€Encaged Pd–Mn Nanocatalysts for CO ₂ Hydrogenation and Formic Acid Dehydrogenation. Angewandte Chemie - International Edition, 2020, 59, 20183-20191.	7.2	175
33	Optimized Synthesis of Agâ€Modified Alâ€Doped SrTiO ₃ Photocatalyst for the Conversion of CO ₂ Using H ₂ O as an Electron Donor. ChemistrySelect, 2020, 5, 8779-8786.	0.7	26
34	Fe-Modified CuNi Alloy Catalyst as a Nonprecious Metal Catalyst for Three-Way Catalysis. Industrial & Engineering Chemistry Research, 2020, 59, 19907-19917.	1.8	15
35	Ni–Pt Alloy Nanoparticles with Isolated Pt Atoms and Their Cooperative Neighboring Ni Atoms for Selective Hydrogenation of CO ₂ Toward CH ₄ Evolution: <i>In Situ</i> and Transient Fourier Transform Infrared Studies. ACS Applied Nano Materials, 2020, 3, 9633-9644.	2.4	24
36	Low-temperature NO oxidation using lattice oxygen in Fe-site substituted SrFeO3â^'î´. Physical Chemistry Chemical Physics, 2020, 22, 24181-24190.	1.3	10

Hiroyuki Asakura

#	Article	IF	CITATIONS
37	Self-Regeneration Process of Ni–Cu Alloy Catalysts during a Three-Way Catalytic Reaction—An <i>Operando</i> Study. ACS Applied Materials & Interfaces, 2020, 12, 55994-56003.	4.0	5
38	Identification of Active Ba Species on TiO ₂ Photocatalyst for NO <i>_x</i> Trapping. Chemistry Letters, 2020, 49, 859-862.	0.7	3
39	Excellent Catalytic Activity of a Pdâ€Promoted MnO x Catalyst for Purifying Automotive Exhaust Gases. ChemCatChem, 2020, 12, 4276-4280.	1.8	11
40	Effect of Surface Reforming via O ₃ Treatment on the Electrochemical CO ₂ Reduction Activity of a Ag Cathode. ACS Applied Energy Materials, 2020, 3, 6552-6560.	2.5	9
41	Photoelectrochemical investigation of the role of surface-modified Yb species in the photocatalytic conversion of CO2 by H2O over Ga2O3 photocatalysts. Catalysis Today, 2020, 352, 18-26.	2.2	5
42	Dynamics of the Lattice Oxygen in a Ruddlesden–Popper-type Sr3Fe2O7â^δ Catalyst during NO Oxidation. ACS Catalysis, 2020, 10, 2528-2537.	5.5	12
43	Effective Driving of Ag-Loaded and Al-Doped SrTiO ₃ under Irradiation at λ > 300 nm for the Photocatalytic Conversion of CO ₂ by H ₂ O. ACS Applied Energy Materials, 2020, 3, 1468-1475.	2.5	56
44	Low-temperature NO trapping on alkali or alkaline earth metal modified TiO2 photocatalyst. Catalysis Today, 2019, 332, 76-82.	2.2	19
45	CO and C3H6 oxidation over platinum-group metal (PGM) catalysts supported on Mn-modified hexagonal YbFeO3. Catalysis Today, 2019, 332, 183-188.	2.2	9
46	Isolated Platinum Atoms in Ni/γ-Al ₂ O ₃ for Selective Hydrogenation of CO ₂ toward CH ₄ . Journal of Physical Chemistry C, 2019, 123, 23446-23454.	1.5	29
47	Sublimation-Induced Sulfur Vacancies in MoS ₂ Catalyst for One-Pot Synthesis of Secondary Amines. ACS Catalysis, 2019, 9, 7967-7975.	5.5	57
48	Quantum Chemical Computation-Driven Development of Cu-Shell–Ru-Core Nanoparticle Catalyst for NO Reduction Reaction. Journal of Physical Chemistry C, 2019, 123, 20251-20256.	1.5	5
49	NOx Oxidation and Storage Properties of a Ruddlesden–Popper-Type Sr3Fe2O7â^î-Layered Perovskite Catalyst. ACS Applied Materials & Interfaces, 2019, 11, 26985-26993.	4.0	23
50	Electrostatic Stabilization of Single-Atom Catalysts by Ionic Liquids. CheM, 2019, 5, 3207-3219.	5.8	131
51	Important Role of Strontium Atom on the Surface of Sr ₂ KTa ₅ O ₁₅ with a Tetragonal Tungsten Bronze Structure to Improve Adsorption of CO ₂ for Photocatalytic Conversion of CO ₂ by H ₂ O. ACS Applied Materials & amp; Interfaces. 2019. 11. 37875-37884.	4.0	9
52	Efficient oxygen storage property of Sr–Fe mixed oxide as automotive catalyst support. Journal of Materials Chemistry A, 2019, 7, 1013-1021.	5.2	12
53	Effect of Cr Species on Photocatalytic Stability during the Conversion of CO ₂ by H ₂ O. Journal of Physical Chemistry C, 2019, 123, 2894-2899.	1.5	7
54	Role of Bicarbonate Ions in Aqueous Solution as a Carbon Source for Photocatalytic Conversion of CO ₂ into CO. ACS Applied Energy Materials, 2019, 2, 5397-5405.	2.5	16

#	Article	IF	CITATIONS
55	Deactivation Mechanism of Pd/CeO ₂ –ZrO ₂ Three-Way Catalysts Analyzed by Chassis-Dynamometer Tests and <i>in Situ</i> Diffuse Reflectance Spectroscopy. ACS Catalysis, 2019, 9, 6415-6424.	5.5	40
56	Self-regeneration of a Ni–Cu alloy catalyst during a three-way catalytic reaction. Physical Chemistry Chemical Physics, 2019, 21, 18816-18822.	1.3	16
57	Atomically Dispersed Pt ₁ –Polyoxometalate Catalysts: How Does Metal–Support Interaction Affect Stability and Hydrogenation Activity?. Journal of the American Chemical Society, 2019, 141, 8185-8197.	6.6	147
58	In situ spectroscopy-guided engineering of rhodium single-atom catalysts for CO oxidation. Nature Communications, 2019, 10, 1330.	5.8	177
59	Local Structure Study of Lanthanide Elements by Xâ€Ray Absorption Near Edge Structure Spectroscopy. Chemical Record, 2019, 19, 1420-1431.	2.9	5
60	Pt–Co Alloy Nanoparticles on a γâ€Al ₂ O ₃ Support: Synergistic Effect between Isolated Electronâ€Rich Pt and Co for Automotive Exhaust Purification. ChemPlusChem, 2019, 84, 447-456.	1.3	12
61	Effect of Thickness of Chromium Hydroxide Layer on Ag Cocatalyst Surface for Highly Selective Photocatalytic Conversion of CO ₂ by H ₂ O. ACS Sustainable Chemistry and Engineering, 2019, 7, 2083-2090.	3.2	32
62	Striking Oxygen-Release/Storage Properties of Fe-Site-Substituted Sr ₃ Fe ₂ O _{7â^Î} . Journal of Physical Chemistry C, 2018, 122, 11186-11193.	1.5	21
63	Recent progress in photocatalytic conversion of carbon dioxide over gallium oxide and its nanocomposites. Current Opinion in Chemical Engineering, 2018, 20, 114-121.	3.8	15
64	Catalytic amino acid production from biomass-derived intermediates. Proceedings of the National Academy of Sciences of the United States of America, 2018, 115, 5093-5098.	3.3	168
65	Flux method fabrication of potassium rare-earth tantalates for CO2 photoreduction using H2O as an electron donor. Catalysis Today, 2018, 300, 173-182.	2.2	24
66	Role of lattice oxygen and oxygen vacancy sites in platinum group metal catalysts supported on Sr ₃ Fe ₂ O _{7â~Î<} for NO-selective reduction. Catalysis Science and Technology, 2018, 8, 147-153.	2.1	29
67	Dynamic Behavior of Rh Species in Rh/Al ₂ O ₃ Model Catalyst during Three-Way Catalytic Reaction: An <i>Operando</i> X-ray Absorption Spectroscopy Study. Journal of the American Chemical Society, 2018, 140, 176-184.	6.6	55
68	Modification of Ga ₂ O ₃ by an Ag–Cr core–shell cocatalyst enhances photocatalytic CO evolution for the conversion of CO ₂ by H ₂ O. Chemical Communications, 2018, 54, 1053-1056.	2.2	53
69	A feasibility study of "range-extended―EXAFS measurement at the Pt L ₃ -edge of Pt/Al ₂ O ₃ in the presence of Au ₂ O ₃ . Journal of Analytical Atomic Spectrometry, 2018, 33, 84-89.	1.6	10
70	Development of Rh-Doped Ga ₂ O ₃ Photocatalysts for Reduction of CO ₂ by H ₂ O as an Electron Donor at a More than 300 nm Wavelength. Journal of Physical Chemistry C, 2018, 122, 21132-21139.	1.5	22
71	Photocatalytic Conversion of Carbon Dioxide over A ₂ BTa ₅ O ₁₅ (A) Tj ETQ Engineering, 2018, 6, 8247-8255.	1 1 0.784 3.2	4314 rgBT /(8
72	Pd/SrFe _{1–<i>x</i>} Ti _{<i>x</i>} O _{3â^î^} as Environmental Catalyst: Purification of Automotive Exhaust Gases. ACS Applied Materials & Interfaces, 2018, 10, 22182-22189.	4.0	13

#	Article	IF	CITATIONS
73	Direct aerobic oxidative homocoupling of benzene to biphenyl over functional porous organic polymer supported atomically dispersed palladium catalyst. Applied Catalysis B: Environmental, 2017, 209, 679-688.	10.8	47
74	Atomically Dispersed Rhodium on Self-Assembled Phosphotungstic Acid: Structural Features and Catalytic CO Oxidation Properties. Industrial & Engineering Chemistry Research, 2017, 56, 3578-3587.	1.8	75
75	Translocation of 133Cs administered to Cryptomeria japonica wood. Science of the Total Environment, 2017, 584-585, 88-95.	3.9	17
76	Which is an Intermediate Species for Photocatalytic Conversion of CO ₂ by H ₂ O as the Electron Donor: CO ₂ Molecule, Carbonic Acid, Bicarbonate, or Carbonate Ions?. Journal of Physical Chemistry C, 2017, 121, 8711-8721.	1.5	54
77	Efficient photocatalytic carbon monoxide production from ammonia and carbon dioxide by the aid of artificial photosynthesis. Chemical Science, 2017, 8, 5797-5801.	3.7	9
78	Effects of the structure of the Rh3+ modifier on photocatalytic performances of an Rh3+/TiO2 photocatalyst under irradiation of visible light. Applied Catalysis B: Environmental, 2017, 205, 340-346.	10.8	8
79	Selective reduction of NO over Cu/Al2O3: Enhanced catalytic activity by infinitesimal loading of Rh on Cu/Al2O3. Molecular Catalysis, 2017, 442, 74-82.	1.0	23
80	Visible-Light Selective Photooxidation of Aromatic Hydrocarbons via Ligand-to-Metal Charge Transfer Transition on Nb ₂ O ₅ . Journal of Physical Chemistry C, 2017, 121, 22854-22861.	1.5	36
81	Drastic improvement in the photocatalytic activity of Ga ₂ O ₃ modified with Mg–Al layered double hydroxide for the conversion of CO ₂ in water. Sustainable Energy and Fuels, 2017, 1, 1740-1747.	2.5	35
82	Thermally stable single atom Pt/m-Al2O3 for selective hydrogenation and CO oxidation. Nature Communications, 2017, 8, 16100.	5.8	545
83	Oxygen Storage Property and Chemical Stability of SrFe _{1–<i>x</i>} Ti _{<i>x</i>} O _{3â^î^} with Robust Perovskite Structure. Journal of Physical Chemistry C, 2017, 121, 19358-19364.	1.5	26
84	CO ₂ capture, storage, and conversion using a praseodymium-modified Ga ₂ O ₃ photocatalyst. Journal of Materials Chemistry A, 2017, 5, 19351-19357.	5.2	38
85	Enhanced oxygen-release/storage properties of Pd-loaded Sr ₃ Fe ₂ O _{7â^î} . Physical Chemistry Chemical Physics, 2017, 19, 14107-14113.	1.3	27
86	Enhancement of CO Evolution by Modification of Ga ₂ O ₃ with Rare-Earth Elements for the Photocatalytic Conversion of CO ₂ by H ₂ O. Langmuir, 2017, 33, 13929-13935.	1.6	43
87	Sodium Cation Substitution in Sr ₂ KTa ₅ O ₁₅ toward Enhancement of Photocatalytic Conversion of CO ₂ Using H ₂ O as an Electron Donor. ACS Omega, 2017, 2, 8187-8197.	1.6	11
88	Highly selective photocatalytic conversion of CO2 by water over Ag-loaded SrNb2O6 nanorods. Applied Catalysis B: Environmental, 2017, 218, 770-778.	10.8	86
89	Stabilizing a Platinum ₁ Singleâ€Atom Catalyst on Supported Phosphomolybdic Acid without Compromising Hydrogenation Activity. Angewandte Chemie, 2016, 128, 8459-8463.	1.6	80
90	Stabilizing a Platinum ₁ Singleâ€Atom Catalyst on Supported Phosphomolybdic Acid without Compromising Hydrogenation Activity. Angewandte Chemie - International Edition, 2016, 55, 8319-8323.	7.2	350

#	Article	IF	CITATIONS
91	Rh nanoparticles with NiO x surface decoration for selective hydrogenolysis of C O bond over arene hydrogenation. Journal of Molecular Catalysis A, 2016, 422, 188-197.	4.8	42
92	Anomalous structural behavior in the metamagnetic transition of FeRh thin films from a local viewpoint. Physical Review B, 2015, 92, .	1.1	13
93	Popping of Graphite Oxide: Application in Preparing Metal Nanoparticle Catalysts. Advanced Materials, 2015, 27, 4688-4694.	11.1	48
94	A theoretical approach to La L1-edge XANES spectra of La complex oxides and their local configuration. Journal of Chemical Physics, 2015, 142, 164507.	1.2	6
95	The support effect on the size and catalytic activity of thiolated Au ₂₅ nanoclusters as precatalysts. Nanoscale, 2015, 7, 6325-6333.	2.8	142
96	Local Structure and L1- and L3-Edge X-ray Absorption Near Edge Structure of Late Lanthanide Elements (Ho, Er, Yb) in Their Complex Oxides. Journal of Physical Chemistry C, 2015, 119, 8070-8077.	1.5	14
97	A Series of NiM (M = Ru, Rh, and Pd) Bimetallic Catalysts for Effective Lignin Hydrogenolysis in Water. ACS Catalysis, 2014, 4, 1574-1583.	5.5	421
98	Order-to-disorder structural transformation of a coordination polymer and its influence on proton conduction. Chemical Communications, 2014, 50, 10241-10243.	2.2	88
99	Highly efficient, NiAu-catalyzed hydrogenolysis of lignin into phenolic chemicals. Green Chemistry, 2014, 16, 2432-2437.	4.6	239
100	Local Structure and La L ₁ and L ₃ -Edge XANES Spectra of Lanthanum Complex Oxides. Inorganic Chemistry, 2014, 53, 6048-6053.	1.9	44
101	Local Structure of Pr, Nd, and Sm Complex Oxides and Their X-ray Absorption Near Edge Structure Spectra. Journal of Physical Chemistry C, 2014, 118, 20881-20888.	1.5	15
102	Ultrathin rhodium nanosheets. Nature Communications, 2014, 5, 3093.	5.8	428
103	Development of Palladium Surfaceâ€Enriched Heteronuclear Au–Pd Nanoparticle Dehalogenation Catalysts in an Ionic Liquid. Chemistry - A European Journal, 2013, 19, 1227-1234.	1.7	73
104	Bifunctionality of Rh ³⁺ Modifier on TiO ₂ and Working Mechanism of Rh ³⁺ /TiO ₂ Photocatalyst under Irradiation of Visible Light. Journal of Physical Chemistry C, 2013, 117, 11008-11016.	1.5	67
105	Rational Design of a Molecular Nanocatalystâ€Stabilizer that Enhances both Catalytic Activity and Nanoparticle Stability. ChemCatChem, 2012, 4, 1907-1910.	1.8	15
106	In situ time-resolved DXAFS study of Rh nanoparticle formation mechanism in ethylene glycol at elevated temperature. Physical Chemistry Chemical Physics, 2012, 14, 2983.	1.3	20
107	In Situ Time-Resolved XAFS Study of the Reaction Mechanism of Bromobenzene Homocoupling Mediated by [Ni(cod)(bpy)]. Journal of Physical Chemistry A, 2012, 116, 4029-4034.	1.1	16
108	Insights into the Formation Mechanism of Rhodium Nanocubes. Journal of Physical Chemistry C, 2012, 116, 15076-15086.	1.5	46

#	Article	IF	CITATIONS
109	Incarceration of (PdO) _{<i>n</i>} and Pd _{<i>n</i>} Clusters by Cageâ€Templated Synthesis of Hollow Silica Nanoparticles. Angewandte Chemie - International Edition, 2012, 51, 5893-5896.	7.2	43
110	Structural Analysis of Group V, VI, and VII Metal Compounds by XAFS. Journal of Physical Chemistry C, 2011, 115, 23653-23663.	1.5	36
111	Structural analysis of group V, VI, VII metal compounds by XAFS and DFT calculation. Journal of Physics: Conference Series, 2009, 190, 012073.	0.3	12
112	In Situ Time-Resolved Energy-Dispersive XAFS Study on Reduction Behavior of Pt Supported on TiO2 and Al2O3. Catalysis Letters, 2009, 131, 413-418.	1.4	22